0026-895X/96/020266-11$3.00/0

MOLECULAR PHARMACOLOGY, 50:266-276 (1996).

Inability to *N*-Glycosylate the Human Norepinephrine Transporter Reduces Protein Stability, Surface Trafficking, and Transport Activity but Not Ligand Recognition

HALEY E. MELIKIAN, SAMMANDA RAMAMOORTHY, CHRISTOPHER G. TATE, and RANDY D. BLAKELY

Graduate Program in Neuroscience, Emory University, Atlanta, Georgia 30322 (H.E.M.), Medical Research Council Laboratory of Molecular Biology, Cambridge, UK CB2 2QH (C.G.T.), and Department of Pharmacology and Center for Molecular Neuroscience, Vanderbilt University School of Medicine, Nashville, Tennessee 37232-6600 (S.R., R.D.B.)

Received December 7, 1995; Accepted April 11, 1996

SUMMARY

The role of *N*-glycosylation in the expression, stability, and ligand recognition by the cocaine- and antidepressant-sensitive human norepinephrine transporter (hNET) was assessed in stably and transiently transfected cell lines. The use of hNET-specific antibodies and the membrane-impermeant biotinylating reagent sulfosuccinimidobiotin establishes that treatment of stably transfected LLC-PK$_1$ cells with tunicamycin depletes surface membranes of mature hNET glycoproteins, which is consistent with a failure of less stable, nonglycosylated subunits to replenish surface compartments. To determine whether *N*-glycosylation plays a direct role in hNET stability, surface expression, and ligand recognition, we mutated the three hNET canonical *N*-glycosylation sites (hNETN184,192,198Q) and transiently expressed the mutant cDNA in parallel with the parental hNET construct in HeLa and COS cells. hNETN184,192,198Q protein exhibited increased electrophoretic mobility (~46 kDa), similar to that of enzymatically *N*-deglycosylated hNET protein, which confirms the use of canonical sites in the second extracellular loop of the transporter. hNETN184,192,198Q protein in HeLa and COS extracts was reduced ~50% relative to hNET protein in parallel transfections, demonstrated to arise from a reduction in transporter half-life, which is consistent with the proposed role of *N*-glycosylation in hNET stability. Both HeLa and COS cells transfected with hNETN184,192,198Q exhibit a significantly greater reduction in transport activity than can be accounted for by losses in either total or surface NET protein. Furthermore, sensitivity of catecholamine transport to unlabeled substrate and antagonists was unchanged in the mutant, suggesting that residual nonglycosylated surface hNETs execute a key step in the transport cycle after ligand recognition with reduced efficiency.

The extracellular concentration of NE bathing synaptic and extrasynaptic adrenergic receptors is regulated by presynaptic NET proteins (1, 2). NETs utilize transmembrane Na^+ and Cl^- gradients to drive NE accumulation inside presynaptic terminals and varicosities, an electrogenic process (3) that is blocked by tricyclic antidepressants and cocaine (4–6) but whose precise mechanisms remain largely undefined. Expression cloning of the hNET cDNA (7) demonstrated that a single cDNA is sufficient to confer antidepressant-sensitive, Na^+-dependent NE transport onto nonneuronal cells. The predicted hNET polypeptide possesses 12 potential TMDs, cytoplasmic NH_2 and COOH termini, and a large hydrophilic loop between TMDs 3 and 4 that contains three consensus sites for *N*-glycosylation. Subsequent homology cloning efforts based on the sequence similarity of NET and a rat brain γ-aminobutyric acid transporter isoform (GAT1) revealed a family of transporter proteins whose predicted structures share multiple topological features (8, 9). In particular, the conservation of multiple *N*-glycosylation sites in the second extracellular loop implies an essential role for *N*-glycosylation for biosynthesis and/or function of all GAT/NET homologs. Heterogeneity in *N*-glycosylation is evident for GAT/NET homologs after transfection into different cell hosts (10–12). Native monoamine transporters also exhibit heterogeneous *N*-glycosylation *in vivo* with regional and developmental variations evident (12–14). Reports of reduced transport activity mediated by GAT/NET homologs after treatment with *N*-glycosylation inhibitors (10, 15) are consistent with an essential role of carbohydrate attachment in

This work was funded by a predoctoral National Institute on Drug Abuse award (H.E.M) and by National Institute on Drug Abuse Award DA07390 (R.D.B.). C.G.T. is the recipient of an Medical Research Council Career Development Award.

ABBREVIATIONS: NE, norepinephrine; hNET; human norepinephrine transporter; NET, norepinephrine transport; TMD, transmembrane domain; TM, tunicamycin; DA, dopamine; RIPA, radioimmunoprecipitation assay; sulfo-NHS-biotin, sulfosuccinimidobiotin; HEPES, 4-(2-hydroxyethyl)-1-piperazineethanesulfonic acid; DMEM, Dulbecco's modified Eagle's medium; MEM, minimal essential medium; SDS, sodium dodecyl sulfate; PAGE, polyacrylamide gel electrophoresis; Ab, antibody; HRP, horseradish peroxidase; ECL, enhanced chemiluminescence.

transporter function, although they fail to distinguish among possible roles of *N*-glycosylation in protein biosynthesis, protein stability, surface trafficking, ligand recognition, and substrate translocation. Synaptosomal DA transporters treated with neuraminidase to remove terminal sialic acid residues exhibit a reduced capacity for amine transport but no apparent shift in substrate recognition (16), suggesting a role for *N*-glycosylation in steps of transport after catecholamine binding. In other membrane proteins, *N*-glycosylation can play an important (17, 18) or an inconsequential (19, 20) role in ligand recognition and transport properties, limiting the scope of generalizations from genetically unrelated transporters.

We described the use of a peptide-directed hNET Ab (N430 Ab) for characterization of hNET protein biosynthesis and *N*-glycosylation in transfected cells (10). Immunoreactive hNET protein in stably transfected LLC-PK_1 cells [LLC-NET (21)] was found to be composed of 80- and 54-kDa species, whereas only a 54-kDa species was evident in transiently transfected HeLa cells. Enzymatic deglycosylation and metabolic inhibition of *N*-glycosylation with TM verified that nonglycosylated hNET protein in both cell types migrates at ~46 kDa. Thus, differential *N*-glycosylation accounts for the variant sizes of hNET glycoproteins in LLC-NET cells as well as the mobility difference observed in comparison with transiently transfected HeLa cells. Pulse-chase metabolic labeling/immunoprecipitation analyses revealed that the 54-kDa species in LLC-NET cells is most likely a metabolic precursor of the 80-kDa form, although significant quantities of the 54-kDa form are measurable at steady state. TM-mediated blockade of *N*-glycosylation in LLC-NET cells reduces both V_{max} of substrate transport and B_{max} of radioligand binding, suggesting that *N*-glycosylation of hNET protein may play an important role in functional expression. Pulse-chase analysis of hNET synthesized in the presence or absence of TM in LLC-NET cells demonstrated that nonglycosylated hNET was markedly unstable and thereby unlikely to contribute to the residual transport activity observed in TM-treated cells. Therefore, we hypothesized that the partial retention of transport activity after TM treatment was a reflection of residual mature hNET at the cell surface, synthesized before the addition of TM, rather than the surface expression of a nonglycosylated transporter of compromised function. Because TM has pleotropic effects on all cellular glycoproteins, even the reduced stability of hNET subunits observed might not reflect a role of hNET glycosylation *per se* in maintaining transporter stability.

In the current study, we used cell surface biotinylation (22, 23) of cells transfected with hNET and hNET that lacked *N*-glycosylation sites and both biosynthetic and functional assays to more definitively explore the role of *N*-glycosylation in hNET trafficking, stability, and ligand recognition. We demonstrated that in LLC-NET cells, the most heavily glycosylated 80-kDa form is enriched in surface membranes relative to cytosolic markers and the 54-kDa hNET intermediate. As predicted, TM treatment of LLC-NET cells significantly depleted the surface pool of 80-kDa material rather than populating these membranes with a nonfunctional nonglycosylated hNET polypeptide, although this effect may have less to do with trafficking efficiency and more to do with compromised protein stability. Thus, although nonglycosylated hNET was less abundant than *N*-glycosylated hNET in transfected cells, it seemed to reach the surface with equivalent, if not enhanced, efficiency. The nonglycosylated hNET that reached the surface seemed, however, to have a compromised capacity to transport, suggesting contributions of the TMD 3–4 loop in conformational changes that mediate translocation of substrates after they bind the carrier.

Experimental Procedures

Materials. Cell culture media (DMEM and MEM) were purchased from Fisher Scientific (Pittsburgh, PA), and fetal bovine serum was obtained from Hyclone Laboratories (Logan, UT). Trypsin, glutamine, penicillin, streptomycin, OptiMEM media, and Lipofectin were obtained from GIBCO BRL (Baltimore, MD). pBluescript SKII$^-$ plasmid was obtained from Stratagene (La Jolla, CA), and pcDNA3 plasmid was from InVitrogen (San Diego, CA). Vaccinia virus-T7 RNA polymerase (vTF7–3) was a gift from Dr. Bernard Moss (National Institute of Allergy and Infectious Diseases, Bethesda, MD). Sulfo-NHS-biotin and monomeric-avidin beads were purchased from Pierce Chemical (Rockford, IL). Monoclonal actin Ab was obtained from Boehringer-Mannheim Biochemicals (Indianapolis, IN). HRP-conjugated goat anti-rabbit Ab, SDS-PAGE molecular weight standards, and SDS-PAGE reagents were from BioRad (Hercules, CA). Tran^{35}S label (1131 Ci/mmol) and methionine/cysteine-deficient media were obtained from ICN Biochemicals (Lisle, IL). [^{3}H]DA (48.6 Ci/mmol), HRP-conjugated sheep anti-mouse Ab, HRP-conjugated streptavidin, ECL reagents, Hybond ECL nitrocellulose membrane, and Hyperfilm ECL were purchased from Amersham (Arlington Heights, IL). Protein A-Sepharose was obtained from Pharmacia (Piscataway, NJ). EcoScint H scintillation fluor was obtained from National Diagnostics (Manville, NJ). Nomifensine was obtained from Research Biochemicals (Natick, MA), and desipramine and TM were purchased from Sigma Chemical (St. Louis, MO). All other materials were obtained from standard commercial vendors and were of the highest grade possible.

Site-directed mutagenesis. Oligonucleotide-directed mutagenesis of hNET cDNA was performed on single-stranded DNA prepared from hNET in pBluescript SKII$^-$ in which the 5′ noncoding region had been removed (pCGT110) and the hNET coding sequence was downstream of the T7 RNA polymerase promoter in a sense orientation. Mutant hNETN192,198Q, which leaves only the first canonical *N*-glycosylation site in the second extracellular loop, was first generated using the sense oligonucleotide 5′-CTTGGAGTACTTGGTGTGTTGGCCAAGCACGGAGCCTTGGA-GGAGCTTGGGGTCGGTACAGTT-3′. Mutant hNETN184,192,198Q, lacking all *N*-glycosylation sites, was subsequently generated by mutagenesis of single-stranded DNA from hNETN192,198Q using the sense oli-gonucleotide 5′-CTTGGGGTCGGTACATTGGGGGCTGTTCCAGGT-3′. Mutants were screened by directly sequencing double-stranded DNA using Sequenase (United States Biochemical Corp., Cleveland, OH) and primers flanking the mutagenic region. The mutated regions were removed using *Xma*I/*Sca*I, ligated into *Xma*I/*Sca*I-digested pCGT110, and resequenced across the ligation region. To place parental and mutant hNETs under the control of a mammalian promoter for expression in COS cells, cDNAs were removed from pBluescript SKII$^-$ constructs via *Eco*RI/*Bam*HI digestion and cloned into *Eco*RI/*Bam*HI-digested pcDNA3 downstream of the cytomegalovirus promoter.

Cell lines and transfections. Cell lines were maintained at 37° in 5% CO_2. HeLa and COS-1 cells were grown in DMEM, and LLC-NET cells were grown in MEM. All media were supplemented with 10% fetal bovine serum, 2 mM glutamine, and 100 units/ml penicillin/streptomycin. HeLa cells were transfected for the times indicated using the vaccinia T7 expression system (100,000 cells in 24-well culture plates) essentially as described (10) but using a 2:1 lipofectin/DNA ratio to increase functional expression levels of mutant hNET. To determine whether reduced temperature during expression would

alleviate reductions in activity observed with hNETN184,192,198Q, transfected cells were maintained at 26° rather than at 37° for the times indicated before assay (always at 37°). For pulse-chase/immunoprecipitation studies, 5×10^5 HeLa cells/well in six-well plates (35-mm wells) were transfected with 5 μg of cDNA using a 3:1 lipofectin/DNA ratio. For surface biotinylation studies, COS cells were transfected 24 hr after plating 2×10^5 cells in six-well dishes using 2 μg of DNA and a 5:1 ratio of Lipofectin/DNA.

Pulse-chase determination of hNET half-life in transiently transfected HeLa cells. HeLa cells were transfected with wild-type hNET or mutant hNETN184,192,198Q. At 3.5 hr after transfection, cells were washed three times in methionine/cysteine-free DMEM and incubated with methionine/cysteine-free DMEM for 30 min at 37°. Deficient medium was removed and replaced with methionine/cysteine-free medium supplemented with Tran^{35}S Label to a final concentration of 500 μCi/ml. After pulse labeling for 10 min at 37°, labeled medium was removed, and cells were washed and then incubated with unlabeled, complete HeLa media. Cells were solubilized at 0.5, 2, 4, 8, and 12 hr in RIPA buffer (10 mM Tris, pH 7.4, 150 mM NaCl, 1 mM EDTA, 0.1% SDS, 1% Triton X-100, 1% Na deoxycholate) for 25 min at 4° and hNET-immunoprecipitated as described previously (10). Quantification was performed by scanning densitometry after establishment of linearity ranges for ECL protein quantification. Density values were plotted for each experiment (four separate experiments with five time points each) as a function of chase time to permit a determination of hNET and hNETN184,192,198Q half-life. Steady state hNET and hNETN184,192,198Q protein (three experiments) were quantified by densitometry of N430 Ab immunoblots (0.5 μg/ml affinity-purified Ab) of transfected cell extracts taken 6 hr after transfection as described previously (10). Data were normalized for loading by subsequent scans of actin immunoreactivity on immunoblots stripped with 100 mM β-mercaptoethanol, 62.5 mM Tris, pH 6.7, and 2% SDS for 30 min at 50°, followed by two 10-min washes in PBS/0.5% Tween-20 at room temperature.

Cell surface biotinylation of hNET in LLC-NET and transiently transfected COS cells. Cell surface biotinylation of LLC-NET cells was performed according to a modification of the procedures described by Sargiacomo *et al.* (22, 23). Stock solutions of sulfo-NHS-biotin (200 mg/ml in DMSO) were stored at −20° before use. Immediately before each experiment, 1 mg/ml sulfo-NHS-biotin solutions were prepared by dilution into ice-cold calcium- and magnesium-supplemented PBS Ca/Mg (138 mM NaCl, 2.7 mM KCl, 1.5 mM KH_2PO_4, 9.6 mM Na_2HPO_4, 1 mM $MgCl_2$, 0.1 mM $CaCl_2$, pH 7.3). Cells were washed four times with ice-cold PBS Ca/Mg, sulfo-NHS-biotin solutions (1 ml) were applied, and cells were gently shaken for 25 min at 4°. Free sulfo-NHS-biotin was removed by washing four times with ice-cold PBS Ca/Mg, and biotinylated cells were solubilized in 1 ml of RIPA buffer. Samples were centrifuged at 20,000 × *g* to pellet nonsolubilized material, and protein determinations were performed on supernatants using the DC Protein Assay (BioRad) with BSA as a standard. Biotinylated proteins were separated from nonbiotinylated proteins by batch affinity chromatography using monomeric avidin beads (250 μl beads/300 μg protein). Before use, irreversible biotin binding sites on beads were blocked with 2 mM biotin in PBS for 15 min at room temperature, and reversible biotin sites were exposed by washing beads three times in 1 ml of 0.1 M glycine, pH 3. Beads were reequilibrated in PBS by washing four times in 1 ml of PBS and then resuspended in PBS to the origin volume. Equivalent amounts of total cell protein were incubated with beads for 1 hr at room temperature, the beads were centrifuged, and samples of the supernatant were stored on ice for subsequent analysis. Beads were washed four times in 1 ml of RIPA buffer, and samples of the final wash were kept on ice for subsequent analysis. Biotinylated proteins were eluted from beads by incubation with Laemmli SDS-PAGE sample buffer for 15 min at room temperature. Samples were not eluted by boiling because of increased aggregation of hNET proteins at elevated temperatures.[1] Duplicate samples were analyzed for biotin and hNET content by immunoblotting on parallel gels. Biotinylated proteins were detected using HRP-conjugated streptavidin (1:5000). Blots were stripped as described above and stored in blocking solution at 4° until they were reprobed. Control actin bands were detected using monoclonal anti-actin Ab (0.5 μg/ml) and HRP-conjugated sheep anti-mouse secondary Ab (1:10,000). Immunoreactive bands were visualized by ECL on Hyperfilm ECL. Quantitative densitometry for assessment of steady state hNET levels in total extracts and surface fractions was normalized for loading using actin bands from total fractions obtained on stripped and reprobed blots. Before quantification, exposures were calibrated with HRP standards and exposure time to ensure that densities used were within the linear range of the film. Results reflect average data across multiple plasmid preparations for both mutant and parental DNAs. In certain experiments, 10 μg/ml TM was added to LLC-NET cells 24 hr before biotinylation to examine the effect of chemical inhibition of *N*-glycosylation (10) on cell surface hNET. COS cell biotinylation experiments were modified (23) to decrease labeling of intracellular proteins and increase recovery of labeled proteins resulting from lower signal/noise ratios (relative to stably transfected LLC-NET cells). In particular, cells were washed twice in PBS Ca/Mg and incubated in PBS Ca/Mg containing 50 mM NH_4Cl on ice for 15 min before solubilization with RIPA and incubation with avidin beads as described above. Biotinylated proteins were eluted with 0.1 M glycine, pH 2.8; neutralized with 1 M Tris, pH 9.5; and diluted to 1× Laemmli sample buffer for SDS-PAGE.

Uptake assays. Transfected HeLa cells and COS cells were washed once and preincubated in buffer (120 mM NaCl, 4.7 mM KCl, 2.2 mM $CaCl_2$, 1.2 mM $MgSO_4$, 1.2 mM KH_2PO_4, 0.18% glucose, 10 mM HEPES, pH 7.4) for 10 min at 37°. Functional studies in HeLa cells were conducted after 6-hr transfections unless otherwise indicated, whereas COS assays were performed 48 hr after transfection. For inhibition studies, antagonists were included in the preincubation step, whereas unlabeled DA was added simultaneously with tracer. Assays were initiated by the addition of [^{3}H]DA (dihydroxyphenyl[1,2-^{3}H]ethylamine) to a final concentration of 100 nM for HeLa cells and 50 nM for COS and incubated (30 min for HeLa, 10 min for COS) at 37°. We used DA instead of NE as a transport substrate because of the reduced cost and increased stability and because the two amines are transported with similar kinetics (8). Uptake was arrested by three 1-ml ice-cold buffer washes, cells were solubilized in 1% SDS, and [^{3}H]DA accumulation was determined by liquid scintillation spectrometry. Specific uptake was determined by subtracting the amount of accumulated [^{3}H]DA in parallel pBluescript SKII$^-$-transfected HeLa cells or -transfected COS cells incubated with 10 μM desipramine (equal to pcDNA3-transfected COS cells). Resulting data were plotted, and IC_{50} values were obtained using nonlinear least-squares curve fits to a four-parameter logistic inhibition equation (Kaleidagraph, Synergy Software). K_I values were derived from IC_{50} values as described by Cheng and Prusoff (24).

Results

The 80-kDa hNET is the predominate surface form in LLC-NET cells. Our first task in examining the impact of *N*-glycosylation on hNET expression was to establish which of two hNET isoforms expressed by LLC-NET cells (21) at steady state reaches the plasma membrane. The membrane-impermeant biotinylating reagent sulfo-NHS-biotin was used to covalently biotinylate cell surface proteins and biotinylated proteins were then isolated from nonbiotinylated proteins by batch affinity chromatography using monomeric avidin-agarose beads (Figs. 1 and 2). Using HRP-conjugated streptavidin (Fig. 1A), biotinylated proteins could be detected

[1] H. E. Melikian, unpublished observations.

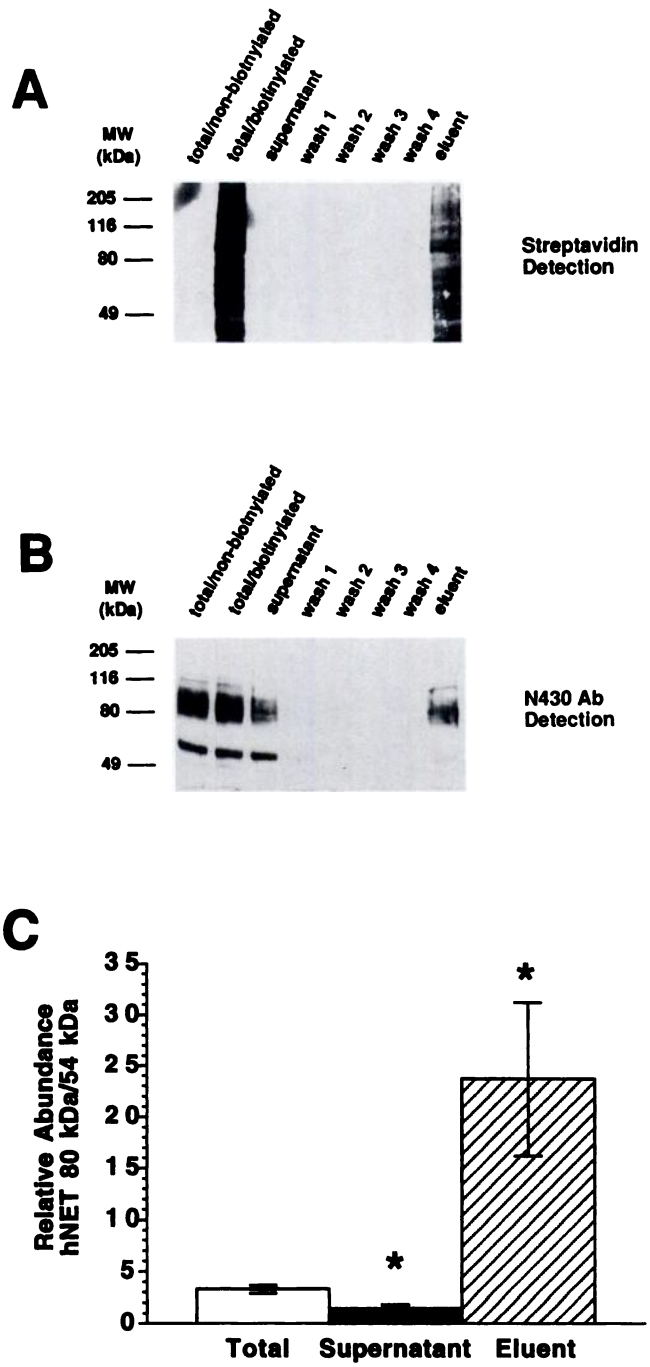

Fig. 1. Cell surface biotinylation of hNET in LLC-NET cells. LLC-NET cells were biotinylated with sulfosuccinimidobiotin, fractionated over monomeric avidin beads, separated by 10% SDS-PAGE, blotted, and probed with (A) HRP-coupled streptavidin or (B) N430 Ab (0.5 μg/ml) as described in Experimental Procedures. Loading in total and supernatant lanes for biotinylated and nonbiotinylated extracts to assess the impact of biotinylation on N430 immunoreactivity was balanced for protein content (25 μg), whereas the entire surface fraction recovered after avidin chromatography (*eluent*) was split between the N430 and streptavidin blots. C, Relative isoform distribution of hNET protein in subcellular fractions. *Bar graph,* ratio of 80-kDa:54-kDa species observed in the total extract (3.25 ± 0.41), supernatant (intracellular pool and nonbiotinylated surface proteins) after batch absorption on avidin agarose (1.45 ± 0.35), and eluent (cell surface pool) after elution from avidin agarose (23.7 ± 7.5). Mean ± standard error values used for ratio determination were obtained by scanning densitometry and normalized to actin immunoreactivity on stripped and reprobed immunoblots (three experiments).

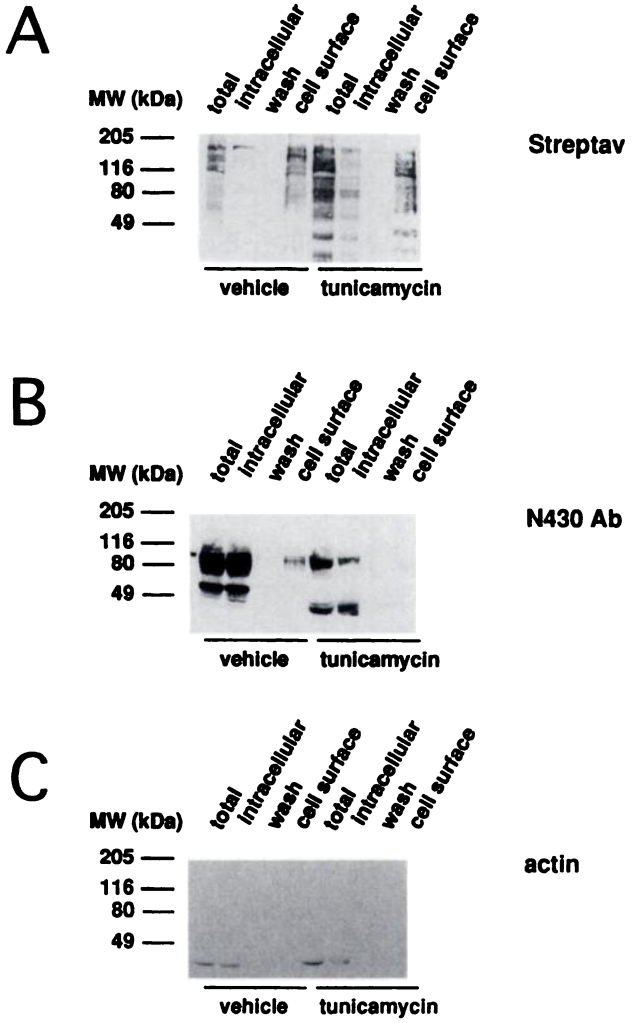

Fig. 2. Effect of TM on cell surface abundance of hNET in LLC-NET cells. After treatment with TM (10 μg/ml, 24 hr) or vehicle, LLC-NET cells were biotinylated, subjected to 10% SDS-PAGE, blotted, and probed with (A) HRP-conjugated streptavidin (1:5000), (B) N430 Ab 0.5 μg/ml, or (C) actin Ab (0.5 μg/ml) as described in Experimental Procedures. Loading in total and intracellular (supernatant) lanes for vehicle and TM was balanced for protein content (33 μg), whereas half of the entire surface fraction recovered after avidin chromatography was split between the N430/actin blot and a parallel streptavidin blot. Actin detection was performed on the N430 blot after stripping.

in whole-cell extracts and eluent (surface) lanes but not in the supernatant (intracellular) fraction. On a parallel blot, N430 Ab detected both 80- and 54-kDa hNET proteins in the total cell extract as described previously (10). Biotinylation had no effect on hNET detection by N430 Ab. The supernatant fraction contained both 80- and 54-kDa forms, although compared with the 54-kDa form, the abundance of the 80-kDa species was reduced relative to the whole-cell extract. hNET in the surface fraction was largely composed of 80-kDa forms. To control for possible permeation of sulfo-NHS-biotin into cells, blots were stripped and reprobed with an Ab directed against the intracellular protein actin. Actin segregated exclusively with the nonbiotinylated proteins, consistent with this material comprising an intracellular fraction along with nonbiotinylated surface proteins (Fig. 2). When levels of immunoreactivity for actin are used to normalize hNET segregation across multiple experiments (three exper-

iments) by densitometry, we could demonstrate an 8-fold ($p < 0.05$, Student's t test) enrichment of the 80-kDa hNET over the 54-kDa species in the cell surface fractions and a depletion of 80-kDa hNET in the intracellular fractions relative to the whole-cell extract (Fig. 1B). Ratios of the 80-kDa form to the 54-kDa form were 3.25 ± 0.41 in the total cell extract, 1.45 ± 0.35 in the intracellular fraction, and 23.7 ± 7.5 in the cell surface fraction.

TM treatment reduces cell surface abundance of 80-kDa hNET in LLC-NET cells. Having established that the 80-kDa hNET form predominates at the cell surface of LLC-NET cells, we next examined potential alterations in intracellular and surface pools after 24-hr TM incubation (Fig. 2), a treatment previously demonstrated to reduce LLC-NET catecholamine transport and membrane radioligand binding capacity. TM treatment results in an overall reduction in 80-kDa hNET, the disappearance of the 54-kDa form, and the appearance of a shorter-lived 46-kDa species (10). Potentially, a nonglycosylated and functionally compromised hNET could replace the 80-kDa material in surface fractions, contributing to reduced substrate transport. Immunoblotting of biotinylated material from control and TM-treated LLC-NET cells revealed, however, that such treatments primarily result in a marked reduction in 80-kDa hNET in the LLC-NET surface fractions (Fig. 2B). The new 46-kDa hNET species, presumed to represent nonglycosylated hNET polypeptide, was absent from surface fractions. No indication of actin biotinylation was found after TM treatment, suggesting that under our incubation conditions, TM does not appreciably permeabilize a significant fraction of LLC-NET cells.

Construction and expression of hNET *N*-glycosylation mutant in HeLa cells. The potential for nonspecific effects of TM, the mixture of residual *N*-glycosylated hNET protein and nonglycosylated polypeptide in membranes from TM-treated LLC-NET cells, and the lack of surface expression of nonglycosylated hNET in surface fractions preclude conclusions as to whether *N*-glycosylation of hNET contributes to ligand recognition and substrate transport. To achieve this goal, we altered the canonical *N*-glycosylation sites in hNET by site-directed mutagenesis and tested the consequences for protein expression, protein stability, surface expression, and ligand recognition in transiently transfected cells. Fig. 3A depicts the location of canonical *N*-glycosylation sites mutated in hNET, and Fig. 3B depicts the electrophoretic mobility of hNET and hNETN184,192,198Q mutant protein in HeLa cells. HeLa cells transfected with hNET cDNA synthesized a 54-kDa polypeptide that can be enzymatically *N*-deglycosylated to yield a 46-kDa polypeptide (10). Consistent with these findings, hNETN184,192,198Q lacking the canonical *N*-glycosylation sites in the TMD 3–4 loop migrates as a polypeptide of 46 kDa (see also Fig. 6). HeLa cells transfected for 6 hr with hNETN184,192,198Q exhibited a substantial (96% loss of function) reduction in [^{3}H]DA accumulation (Table 1). Similar single-point assays conducted on hNETN184,192,198Q-transfected COS cells revealed ~30% of the activity of hNET-transfected cells (430.4 ± 44.0 versus 1366.1 ± 47.5 fmol/10^6 cells/min, seven experiments). Saturation analyses of [^{3}H]DA transport in COS cells revealed monophasic kinetics for both parental and mutant hNET and no significant alteration in substrate K_m (168.4 ± 33.4 versus 183.7 ± 93.2 nM). However, we did observe a significant reduction in V_{max} (977.7 ± 65.4 versus 471.9 ± 81.7 fmol/min/10^6 cell). Because mutant transport activity in COS cells was not reduced to the degree seen in HeLa cells and COS cells were always assayed 2 days after transfections, we tested to determine whether longer transfection times would elevate the relative activity of hNETN184,192,198Q in HeLa cells. An increase in the transfection time at 37° to 16 hr increased the activity of hNETN184,192,198Q relative to hNET, but a 90% loss of function was still evident (Table 1), suggesting that factors other than expression time contribute to differential activity losses in the two systems. Reduced efficiency of surface trafficking of mutant membrane proteins arises, in some cases, from a temperature-sensitive intracellular retention of otherwise functional protein (25). We thus tested whether hNETN184,192,198Q function in HeLa cells could be rescued by a reduction in temperature during synthesis. Cells were transfected according to our standard protocol and then shifted for 6 hr to a reduced temperature (26°) before assay. Transport was assayed at 37° in all cases. In this paradigm, similar [^{3}H]DA accumulation was observed for hNET- and hNETN184,192,198Q-transfected cells (Table 1); however, the overall expression level for both cDNAs was very low and close to that seen with nontransfected cultures. Maintenance

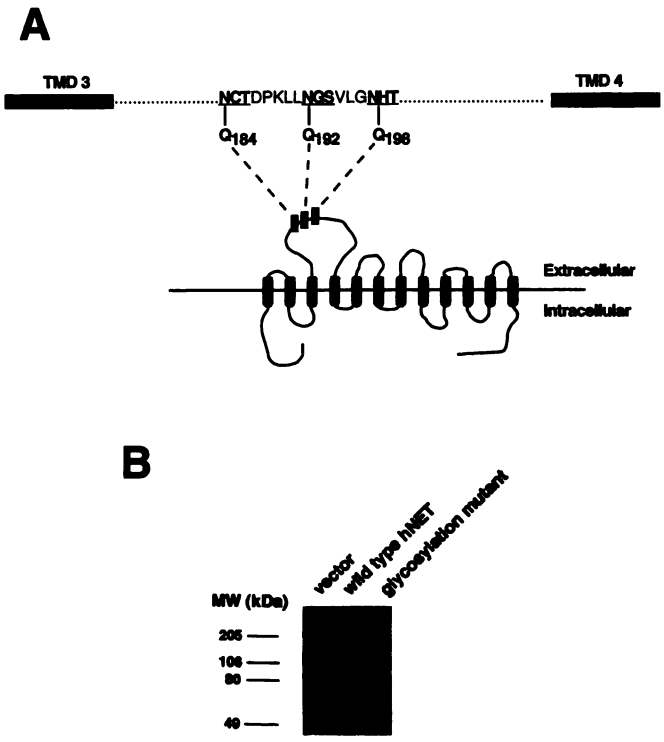

Fig. 3. Site-directed mutagenesis of *N*-glycosylation sites in hNETN184,192,198Q. A, Diagrammatic presentation of the location of canonical *N*-glycosylation sites in topological model for hNET protein. *Barrels*, putative TMDs; *black boxes*, relative location of *N*-glycosylation sites between TMDs 3 and 4; *underline*, canonical *N*-glycosylation motifs modified in hNETN184,192,198Q. B, Immunoblot of total cell extracts (20 μg) of hNET and hNETN184,192,198Q-transfected HeLa cells. Cells were solubilized 6 hr after transfection and underwent SDS-PAGE (10%) and immunoblot with N430 Ab (0.5 μg/ml) as described in Experimental Procedures. The particular immunoblot chosen is presented to emphasize migration differences between the two species and does not accurately reflect relative abundance of hNETN184,192,198Q protein as normalized by actin reprobing, which on average was decreased to 45 ± 13% of that observed in hNET-transfected cells (four experiments).

TABLE 1

Desipramine-sensitive DA uptake in transfected HeLa cells

Transport activity measurements for hNET and *N*-glycosylation mutant hNET (hNETN184,192,198Q) in transfected HeLa cells. Assays were performed as described in Experimental Procedures either 6 or 16 hr after transfection. Assays were performed in triplicate at 37° after 26° or 37° transfection periods. All cells received vaccinia-T7 virus for 2 hr at 37° before transfection. "Nonspecific" for all assays was defined by parallel incubations with 10 μM desipramine and was equal to that obtained with vector-transfected HeLa cells. Values are mean ± standard error based on the results of three experiments. hNET/hNET mutant represents ratio of activities at the respective time and temperature.

	Expression time temperature			
	6 hr		16 hr	
	26°	37°	26°	37°
	fmol/10⁶ cells/min			
cDNA				
hNET	2.9 ± 0.82	476.8 ± 9.3	12.3 ± 0.38	1164.6 ± 41.7
hNET mutant	2.0 ± 0.27	19.7 ± 0.6	2.2 ± 0.16	113.3 ± 3.4
hNET/hNET mutant[a]	1.45	24.2	5.6	10.3

[a] Nonspecific accumulation was as follows: 6 hr, 26° = 7.9 fmol/10⁶ cells/min; 6 hr, 37° = 13.8 fmol/10⁶ cells/min; 16 hr, 26° = 4.8 fmol/10⁶ cells/min; 16 hr, 37° = 21.8 fmol/10⁶ cells/min.

of cultures at 26° for longer periods of time (16 hr) resulted in an elevated level of activity for hNET-transfected cells but failed to reveal a significant rescue of function for hNETN184,192,198Q.

HeLa cells expressing hNET *N*-glycosylation mutant exhibit reduced catecholamine uptake but normal ligand recognition. We next sought to determine whether the reduced transport activity of hNETN184,192,198Q-transfected HeLa cells arises from alterations in key aspects of the substrate binding site. Thus, we determined whether the substrate DA or two competitive, molecularly distinct hNET antagonists exhibit altered potency for inhibition of [^{3}H]DA transport. As shown in Fig. 4, A–C, both parental and mutant hNET activities were equivalently sensitive to inhibition by DA (K_I = 0.30 ± 0.10 versus 0.28 ±.10 μM), the tricyclic desipramine (K_I = 1.26 ± 0.57 versus 1.45 ± 0.86 nM), and the isoquinoline nomifensine (K_I = 4.96 ± 1.01 versus 4.88 ± 1.41 nM). Similarly, transfected COS cells exhibited a transport activity that was 32% of that of hNET-transfected cells (430.4 ± 44.0 versus 1364.1 ± 47.5 fmol/min/10⁶ cells, seven experiments, 50 nM substrate), yet antagonist sensitivity remained intact (data not shown). Thus, the loss of functional activity seen with hNETN184,192,198Q is unlikely to arise from improper ligand recognition.

Transfection of hNET *N*-glycosylation mutant yields hNET protein with decreased protein stability. To determine whether reduced catecholamine transport activity of hNETN184,192,198Q-transfected cells could simply be explained by decreased stability and lower polypeptide levels, autoradiograms of immunoblots from hNET- and hNETN184,192,198Q-transfected HeLa and COS cells were scanned by densitometry and normalized for actin content on stripped and reprobed blots. We found hNETN184,192,198Q protein to be less abundant in whole-cell extracts of transfected HeLa (45 ± 13% of hNET, 6-hr transfection) and COS cells (54.6 ± 7.0% of hNET). The lowered steady state level of hNET protein derived from the complete *N*-glycosylation mutant could be accounted for by a problem with transporter translation and/or stability. To examine this issue, we compared the stabilities of hNET and hNETN184,192,198Q in transiently transfected HeLa cells by pulse-chase metabolic labeling followed by immunoprecipitation. HeLa cell hNET bands from pulse-chase immunoprecipitations underwent scanning densitometry, absolute and relative absorbances were plotted versus chase time, and protein half-lives were calculated from exponential decay curves fit to the data. Fig. 5, A and B, presents a representative autoradiogram and exponential fit, respectively, used to evaluate hNET protein turnover in transfected HeLa cells. Although absolute levels of hNET protein recovered 30 min after the chase were reduced in the mutant (81.4 ± 15.7 relative to hNET, four experiments), this reduction could not account for the reduction in total hNET protein at 6 hr after transfection, assuming that the subsequent degradation rates were equivalent. Analysis of the full biosynthetic course of these proteins reveals that hNETN184,192,198Q protein turnover is significantly accelerated, with a protein half-life reduced by 56 ± 19% ($p < 0.05$, Student's t test) compared with hNET (2.8 ± 0.9 versus 5.0 ± 0.6 hr, four experiments).

Reduction in surface expression of glycosylation mutant does not account for reduced transport. Although diminished, the reduction in total hNETN184,192,198Q protein in HeLa and COS cell extracts fails to account for the reduced transport activity (96% loss in HeLa, 69% loss in COS). Because the functional pool of hNET protein resides at the cell surface, we wanted to determine how the relative abundances of hNET and hNETN184,192,198Q in surface membranes compare with the representation in total cell extracts and thus whether the efficiency of trafficking hNETN184,192,198Q to the cell surface was reduced relative to hNET, accounting for a greater loss of transport than protein. Unfortunately, an unacceptable level of background actin biotinylation of vaccinia-T7-infected HeLa cells prohibited us from estimating the relative surface compartmentation of the two proteins in HeLa cells. We also examined other nonviral transient transfection techniques for HeLa cells (data not shown) but found hNET expression to be too low for surface analysis. Biotinylation of hNET and hNETN184,192,198Q expressed in COS cells (Fig. 6A), however, could readily be achieved without significant biotinylation of intracellular actin (Fig. 6B). Quantification of COS cell biotinylation experiments is presented in Table 2. In unfractionated extracts of hNET-transfected COS cells, 46- and 54-kDa forms are detected by N430 Ab in roughly equivalent abundance. The 46-kDa species comigrates with the single species evident in total extracts from hNETN184,192,198Q-transfected COS cells. Surface fractions of hNET-transfected COS cells contain both 46- and 54-kDa forms, in essentially similar ratios as the total cell extract, whereas hNETN184,192,198Q surface pools con-

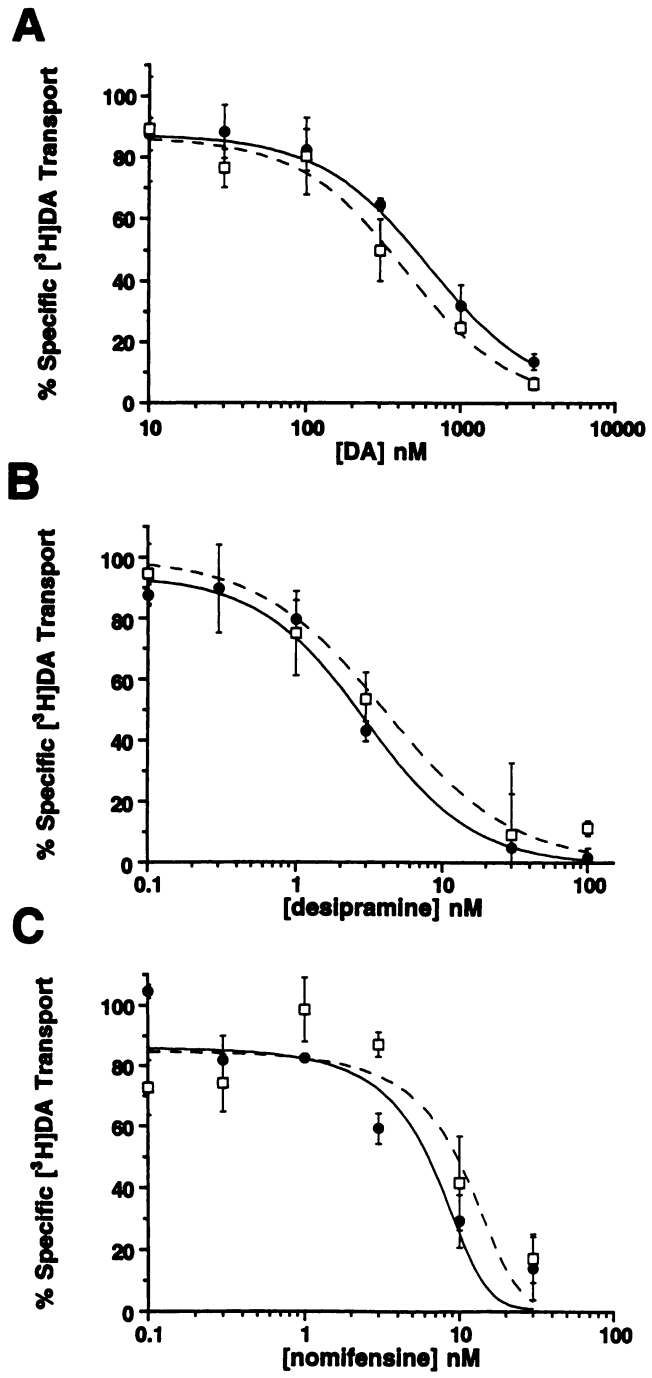

Fig. 4. hNET and hNETN184,192,198Q substrate and antagonist sensitivity. Uptake studies were performed on HeLa cells 6 hr after transfection with either wild-type (●) or glycosylation mutant (□) hNET. Data for DA (A), desipramine (B), and nomifensine (C) incubations are plotted as a percentage of specific [^{3}H]DA uptake. Nonspecific accumulation was determined from transfections with pBluescript SKII$^-$, and the values were subtracted from the total accumulation to determine specific transport. Representative experiments performed with hNET and hNETN184,192,198Q transfected in parallel cultures are presented for each compound.

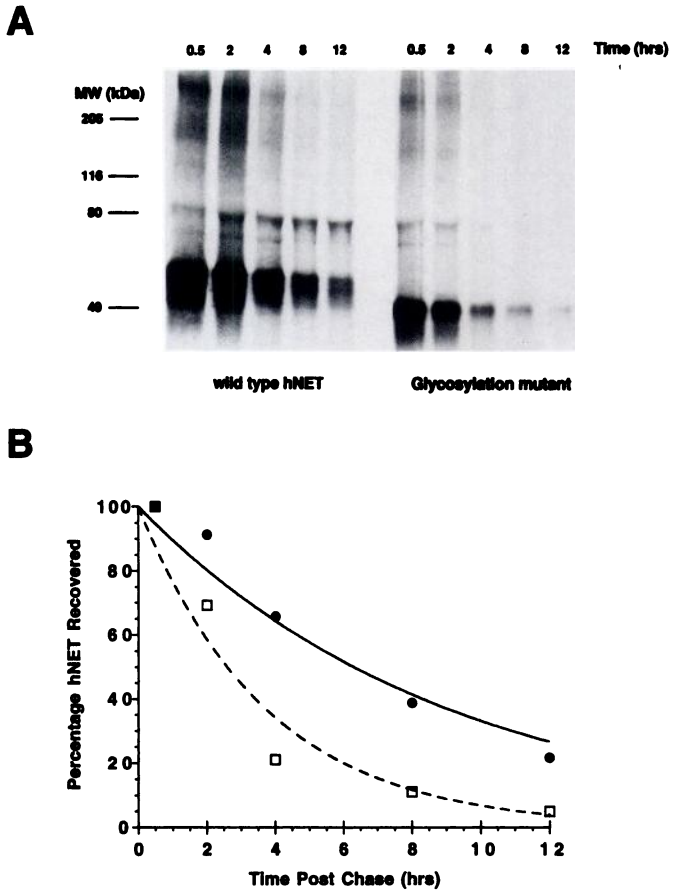

Fig. 5. Pulse-chase estimation of hNET and hNET N184Q, N192Q, N198Q stability in transfected HeLa cells. A, HeLa cells were transfected with either wild-type hNET or hNETN184,192,198Q cDNA, pulse-labeled, incubated with unlabeled media for the indicated times, immunoprecipitated with N430 Ab, and autoradiographed as described in Experimental Procedures. B, Plot of band intensities, expressed as a percentage of initial time point, plotted as a function of time and fit by exponential decay curve. Densities across the experiment were expressed as the fraction remaining after chase with unlabeled media. Average half-life for hNET and hNETN184,192,198Q proteins was determined to be 5.0 ± 0.6 and 2.8 ± 0.9 hr, respectively (mean value from four experiments separate experiments with five time points each).

tain only the 46-kDa form. N430 Ab immunoreactive protein in surface fractions of hNETN184,192,198Q-transfected COS cells was reduced to 71% of the level recovered in surface pools of hNET transfected cells, whereas activity loss should predict a drop to 48% of the surface hNET pool. Thus, reduction in surface trafficking of hNET protein alone cannot account for the loss of transport activity. Indeed, comparison of the efficiency by which nonglycosylated 46-kDa proteins derived from the two cDNAs appear in surface pools (amount in surface/amount in total extract) demonstrates that if anything, the presence of a canonical *N*-glycosylation site reduces the efficiency by which NET proteins populate surface fractions of transfected COS cells.

Discussion

N-glycosylation of hNET is a feature of the biosynthesis of the transporter in transfected HeLa and LLC-NET cells (10). In LLC-NET cells, 80- and 54-kDa species were detected by hNET-specific Abs, with pulse-chase studies indicating that the 54-kDa species is a short-lived biosynthetic precursor of the 80-kDa protein. We estimated the half-life of the 80-kDa form to be ~24 hr, whereas the 54-kDa form is either further processed or degraded 4 hr after translation. In HeLa cells, we found only a 54-kDa form. This form shares a common

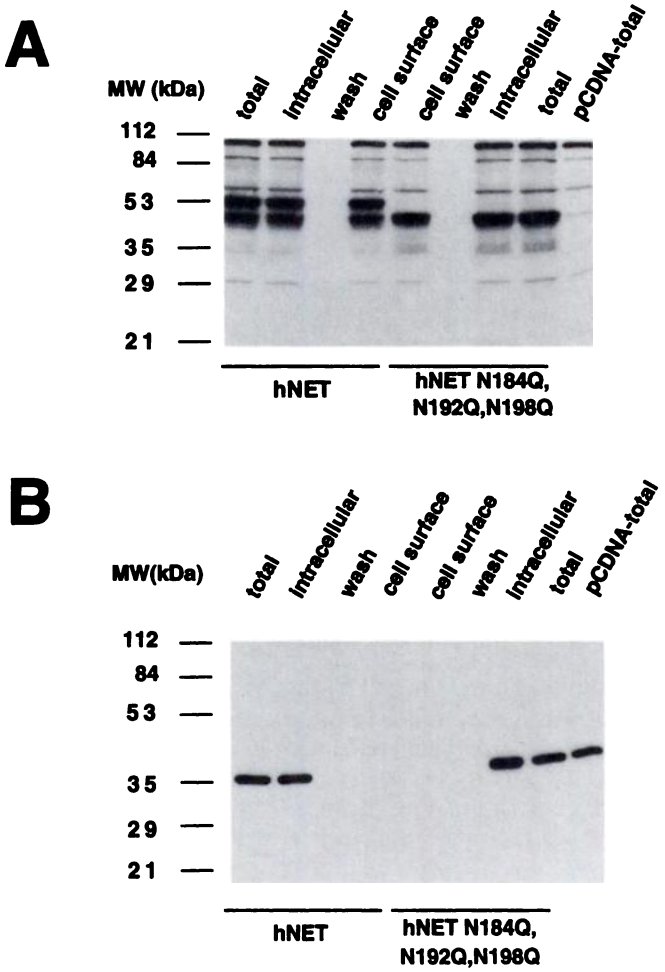

Fig. 6. Cell surface labeling of hNET and hNETN184,192,198Q in transiently transfected COS cells. COS cells were transfected with hNET and hNETN184,192,198Q cDNAs in pcDNA3 or with pcDNA3, and cell surface biotinylation was performed 48 hr after transfection as described in Experimental Procedures. Total and intracellular fractions were balanced for protein before loading loading (5 μg/lane), whereas the entire sample eluted from the avidin beads was loaded as the biotinylated, cell surface fraction. Blots were first probed with N430 Ab (0.5 μg/ml) and then stripped and reprobed with actin Ab (0.5 μg/ml) before autoradiography and scanning densitometry (Table 2).

core size with the LLC-NET hNET proteins of 46 kDa, indicating that the two cell types *N*-glycosylate the transporter to different extents. No pharmacological differences between hNET expressed in these two environments were found, suggesting that *N*-glycosylation might have contributed more to biosynthetic rates, subcellular compartmentation, or substrate translocation rates. Indeed, we noted that TM block of *N*-glycosylation in LLC-NET cells rendered hNET unstable and depleted membranes of hNET antagonist binding capacity. We surmised that the TM reduction in catecholamine transport arose from reduced surface expression of hNET proteins rather than from an important role of *N*-glycosylation in ligand binding or substrate translocation. Although these initial findings suggest a role of *N*-glycosylation in maintaining protein stability, we were unable to directly assess whether *N*-glycosylation *per se* plays a role in hNET stability, surface trafficking, and/or ligand recognition. First, TM treatment blocks *N*-glycosylation of all cellular glycoproteins, and therefore alterations in stability and transport activity might arise secondarily as a result of perturbations in an unrecognized, but essential, protein. Even with this concern discounted, transport activity in TM-treated LLC-NET cells may be dominated by residual *N*-glycosylated material synthesized before TM addition, still at the cell surface. Radiolabeled antagonist binding to TM-treated cell membranes presumably reflects a contribution of both *N*-glycosylated (before TM) and non-*N*-glycosylated (after TM) hNET proteins, which clouds the issue. In our study, direct enzymatic deglycosylation of LLC-NET membranes proved to be of no use in this analysis because enzymatic treatments sufficient to remove all *N*-linked sugars from hNET essentially abolished hNET ligand recognition, which is consistent either with a role of *N*-glycosylation in antagonist binding or, more likely, a nonspecific disruption of membrane proteins under the rather harsh enzymatic conditions that were used. Finally, we lacked the ability to distinguish cell surface hNET from intracellular hNET because available radioligands are highly membrane permeant, and thus caution is necessary when translating data from whole-cell binding to surface density estimates.

In the current study, we implemented a cell surface biotinylation paradigm (22) and established that the 80-kDa hNET synthesized in LLC-NET cells is the predominate surface form and thus largely accounts for the catecholamine transport activity of these cells. Intracellular actin, blotted in parallel, appeared only in nonfractionated or intracellular fractions. The low, but detectable, level of 54-kDa hNET in the surface fraction may indicate a limited accessibility of this form to surface trafficking pathways in overexpression systems or a minor degree of accessibility of sulfo-NHS-biotin to the intracellular compartment of lysed or otherwise damaged cells. With the ability to identify the surface hNET responsible for activity in LLC-NET cells, we were able to validate that TM treatment reduces activity primarily through a depletion of the cell surface 80-kDa form and not through the substitution of a nonfunctional subunit. The 46-kDa nonglycosylated protein synthesized after TM treatment fails to reach the cell surface in significant quantities in these cells, most likely due to its marked instability (10). Thus, functional experiments that report changes in transport capacity of hNET or homologs after chemical treatments to block *N*-glycosylation (15, 26) probably report function of a reduced population of *N*-glycosylated transporter still present at the cell surface rather than the importance of *N*-glycosylation in ligand recognition or transport kinetics *per se*. Recently, investigators studying the effects of TM on the homologous GLYT1 transporter expressed in COS cells (27) also inferred that TM results in the formation of an unstable, nonglycosylated polypeptide that is unlikely to populate surface membranes efficiently.

To directly assess the role of *N*-glycosylation in hNET expression, stability, surface localization, and ligand recognition, we used site-directed mutagenesis to generate an hNET mutant devoid of all canonical *N*-glycosylation sites (hNETN184,192,198Q). Mutant hNET polypeptides expressed in HeLa and COS cells migrate on SDS-PAGE at 46 kDa, essentially the size previously observed in enzymatic deglycosylation experiments (10) and after TM treatment (data not shown). Confirmation that the *N*-glycosylation sites in this domain are used supports that this domain is extracellular in the present topological model for hNET (7) be-

TABLE 2

Distribution of glycosylated and nonglycosylated hNET proteins in transfected COS cells

Estimation of total and surface representations of glycosylated and nonglycosylated hNET proteins in hNET-transfected COS cells and the distribution of *N*-glycosylation mutant (hNETN184,192,198Q) protein, quantified in parallel transfections. Cells were transfected, biotinylated, harvested, and immunoblotted as described in Experimental Procedures. Pool fraction represents the relative representation (percentage ± standard error based on three experiments) of each isoform in the pool listed. Surface recovery represents the distribution of hNET proteins in surface fractions relative to abundance in the total extract. Mutant recovery reflects the fraction of 46-kDa protein present in hNETN184,192,198Q-transfected COS cells relative to the amount of hNET protein (46 + 54 kDa) in hNET-transfected COS cells. Mutant surface enrichment reflects the fraction of surface/total NET protein for hNETN184,192,198Q-transfected COS cells divided by the same ratio achieved in hNET-transfected COS cells. Values are average ± standard error based on three separate experiments with all experiments normalized by actin content.

cDNA	Pool	Isoform	Pool fraction	Surface recovery	Mutant recovery	Mutant surface enrichment
		kDa			%	
hNET						
	Total	46	51.1 ± 1.6	N.A.	N.A.	N.A.
		54	48.9 ± 1.6	N.A.	N.A.	N.A.
	Surface	46	49.9 ± 1.8	0.69 ± 0.05	N.A.	N.A.
		54	51.1 ± 1.8	0.67 ± 0.05	N.A.	N.A.
hNETN184,192,198Q						
	Total	46	100	N.A.	54.6 ± 7.0[b]	N.A.
	Surface	46	100	0.91 ± 0.04[a]	70.9 ± 3.0[c]	133.2 ± 14.0

[a] Significantly increased surface recovery ($p < 0.05$, Student's *t* test) of 46-kDa NET protein relative to protein in the total extract compared with hNET-transfected cells.

[b] Significantly reduced immunoreactive NET protein ($p < 0.05$, Student's *t* test) in hNETN184,192,198Q-transfected COS cells (46 kDa) compared with hNET-transfected COS cells (46 + 54 kDa).

[c] Significantly greater level ($p < 0.05$, Student's *t* test) of NET protein in surface pool of hNETN184,192,198Q-transfected COS cells than expected from change in transport V_{max} (48 ± 3.2%, three experiments), assuming that glycosylated and nonglycosylated NET isoforms are equivalently functional.

N.A. = not applicable.

cause, with few exceptions (28), luminal enzymes are responsible for *N*-glycosylation (29, 30). When HeLa and COS cell immunoblots were normalized for actin content, we found hNETN184,192,198Q levels to be ~50% of those in hNET-transfected cells, findings that were consistently observed and that spanned multiple plasmid preparations. This reduction in steady state protein was largely accounted for by a ~50% reduced half-life of the mutant protein. Our previous study (11) on the rat serotonin transporter expressed in Sf9 cells also indicated that failure to *N*-glycosylate this closely related hNET homolog reduced protein levels, accounting for losses in membrane antagonist (RTI-55) binding capacity. Reductions in stability have been seen for other transporters lacking *N*-glycosylation sites. For example, mutant GLUT1 glucose transporters exhibit a reduced protein half-life (31), and mutant GLYT1 glycine transporters achieve markedly reduced steady state levels in transfected cells, possibly because of increased turnover (27). *N*-glycosylation may be an indication that hNET has folded correctly, restricting its access to intracellular proteases responsible for ensuring fidelity in protein topology. The greater reduction in half-life of hNET protein in TM-treated LLC-NET cells relative to that found with hNETN184,192,198Q may reflect differences in the cellular context of expression, the increased stability of the 80-kDa form not produced in HeLa and COS cells, nonspecific effects of TM, or a combination. More importantly, the reduced steady state level of hNET protein in HeLa and COS cells does not explain the greater functional loss observed in transport assays. Rather, it seemed that the mutation must either reduce cell surface trafficking efficiency or compromise specific aspects of the transport mechanism over and above its effects on hNET stability.

We could find no evidence for reduced surface trafficking of the nonglycosylated hNET protein beyond that expected from loss of protein stability. Defects in function in HeLa cells could not be overcome by maintenance of low temperatures during expression, a strategy that does restore surface expression of some intracellularly retained, but otherwise functional, mutant proteins such as the CFTR protein (25). More directly, we found that hNETN184,192,198Q protein actually is found in surface fractions to a *greater* extent than would be expected from the reduction in protein in whole-cell extracts. The increased recovery of 46-kDa protein in hNETN184,192,198Q-transfected COS cell surface pools relative to either the 46-kDa or the 54-kDa form in hNET-transfected cells could indicate that the surface trafficking machinery is saturated to a greater degree for hNET because total levels of protein exceed those achieved with the mutant. Thus, more newly synthesized hNET may be trapped inside the cell, reducing the fractional recovery of hNET proteins in surface membranes. Alternatively, *N*-glycosylation may be nonessential, but rate limiting, for surface trafficking. The latter explanation requires that glycosylation of the 54-kDa form can limit the appearance of the 46-kDa form because in hNET-transfected cells, both forms exhibit reduced surface recovery relative to hNETN184,192,198Q protein. This could occur if hNET assembles as a multimer after *N*-glycosylation, a possibility to explore in future studies. Saturation experiments reveal similar monophasic kinetics in COS cells when 46- and 54-kDa forms are present (hNET) or when only the 46-kDa form is synthesized (hNETN184,192,198Q). The presence of more hNET protein in surface pools than predicted from losses of activity suggests a role for *N*-glycosylation in specific steps in the transport of substrates across the plasma membrane. It should also be noted that we recovered only ~1% of total immunoreactive NET protein in surface fractions. Although this finding cannot be taken as a quantitative statement of the absolute compartmentation of hNET in surface fractions due to inefficiencies with the biotinylation procedure (23), we (10) and others (31a) have previously noted that significant quantities of hNET protein remain intracellular in heterologous expression systems.

Current models (32, 33) for ion-coupled neurotransmitter transport involve high affinity binding of substrate from the extracellular medium, reorientation of domains in the carrier to expose the binding site to the cytoplasm, release of transmitter, and finally reorientation of the binding site to initiate subsequent cycles of transport. In theory, *N*-glycosylation

could contribute to any or all of these steps, although the likely presence of added sugars on extracellular domains immediately raises the question of ligand recognition. Fortunately, a degree of function suitable for inhibitor characterization is retained by the mutant. We could detect no reductions in sensitivity of transport derived from hNETN184,192,198Q to the substrate DA or two structurally dissimilar antagonists. Similarly, Tate and Blakely (11) demonstrated that nonglycosylated serotonin transporter exhibits no alteration in K_M for serotonin uptake or K_D for binding of the cocaine analog [^{125}I]RTI-55. Rather than an alteration in ligand recognition, we suggest that the efficiency by which bound substrates are transported across the membrane in the mutant seems to be compromised. In support of our conclusions, Zaleska and Erecińska (16) also found evidence in synaptosomes for compromised catecholamine translocation without perturbation of amine recognition by using neuraminidase treatment to remove sialic acid from the DA transporter. Preliminary studies involving chimeras in the TMD 3–4 loop of the serotonin transporter also indicate reduced transport activity with little or no loss in surface pools (6), which is consistent with a role of this domain in conformational changes required for an important step in the translocation cycle subsequent to ligand binding. Additional studies are required to determine whether the compromised step is one of inward substrate transfer or reorientation of an unloaded carrier for subsequent cycles, either of which could reduce overall transport rates. Because we measure activity from a population of surface carriers, it is also possible that a fraction of the mutant carriers are completely inactive rather than the total population exhibiting reduced substrate translocation rates. Paradigms reporting the activity of single hNET molecules (33a) may provide insight into this possibility.

The presence of nonglycosylated hNET protein with reduced translocation efficiency in surface fractions may also explain the quantitative discrepancy between HeLa and COS cell reductions in catecholamine transport. HeLa cells exhibit a greater reduction in activity with hNETN184,192,198Q despite the fact that COS and HeLa cells have essentially the same percentage of reduction in immunoreactive NET protein at steady state. However, COS cells transfected with hNET cDNA possess a significant pool of nonglycosylated 46-kDa protein, whereas HeLa cells do not, and in COS cells, the 46-kDa protein can be shown to reside at the surface, where it presumably contributes only fractional transport activity. Were all of the COS surface protein the 54-kDa form, as it is in hNET-transfected HeLa cells, COS cells would exhibit significantly greater transport activity, and the drop seen with the mutant would then appear larger as well. Although we lack knowledge of the efficiency for surface trafficking in HeLa cells due to limitations with vaccinia-T7 expression, our COS data indicate that at a minimum, a ~30% reduction in catalytic activity for the nonglycosylated protein would explain our transport data. Differences between our results and those for the nonglycosylatable GLYT1 glycine transporter, for which surface trafficking rather than catalytic efficiency may be perturbed (27), could reflect the use of four instead of than three *N*-glycosylation sites in the TMD 3–4 loop of GLYT1. Notably, a partially *N*-glycosylated GLYT1 transporter (lacking two of four *N*-glycosylation sites) exhibits reduced glycine uptake after transfection despite little if any reduction in surface protein that can be labeled.

hNET can be expressed in heterologous expression systems from a single cDNA (7). The coding sequence predicted for hNET, like that of other transporter members of the *hNET/GAT1* gene family, bears multiple sites for *N*-glycosylation on a large hydrophilic loop between putative TMDs 3 and 4. Although we have established that *N*-glycosylation occurs at canonical sites in the TMD 3–4 intervening loop of hNET, we have not attempted to subdefine the *N*-glycosylation status. However, high mannose *N*-glycosylation, the precursor to more complex glycolytic processing, typically adds ~2.5 kDa of mass to polypeptides per *N*-glycosylation site used (34). We estimate that there is ~8 kDa of *N*-glycosylation present on 54-kDa forms of hNET in LLC-NET, HeLa, and COS cells, suggesting that each of the three canonical sites of hNET may be processed by high mannose glycosylation. In support of this idea, LLC-NET cells convert the 54-kDa form to a more highly glycosylated 80-kDa form that is sensitive to PNGase F digestion (10). Retention of the first *N*-glycosylation site of hNET in hNETN192,198Q leads to a less severe, although significant (~60%), reduction in transport in HeLa cells (data not shown). In contrast to our studies with COS and HeLa cells, stably transfected LLC-PK1 (10) and human embryonic kidney 293 cells (4), like the spontaneous neuroblastoma SK-N-SH (35), synthesize significant quantities of 80-kDa NET, suggesting that transient expression, rather than heterologous expression *per se*, may limit more complex *N*-glycolytic processing. Similarly, mutational analysis of individual *N*-glycosylation sites of the homologous glycine transporter GLYT1 (27) and serotonin transporter (11) reveals a stepwise increase in both electrophoretic mobility and functional expression, suggesting contributions to expression from each of the *N*-glycosylated positions. Terminal *N*-glycolytic processing is well known to vary by cell type and as a function of development (29, 36). Different tissues seem to *N*-glycosylate biogenic amine transporters to different extents (12, 37, 38), and although investigators have questioned the contributions of differential post-translational processing to functional properties, the functional significance of these distinctions has not been clarified. Blockade of cellular *N*-glycosylation with TM reduces catecholamine transport capacity for NET-expressing cell lines as well as transfected cells, results we can now interpret as the result of loss of surface carriers. Our data also suggest that changes in *N*-glycosylation patterns seen for homologous carriers *in vivo* may have an impact on substrate translocation rates per unit of protein, with functional consequences for amine clearance at sites of expression or during development.

Acknowledgments

We thank Dr. Charles Saxe, Dr. Eric Barker, and Dr. Gary Rudnick for helpful discussions during the conduct of these studies and preparation of the manuscript and Namita Patel and Kimberly Moore for excellent technical support.

References

1. Iversen, L. L. Role of transmitter uptake mechanisms in synaptic neurotransmission. *Br. J. Pharmacol.* 41:571–591 (1971).
2. Trendelenburg, U. The TiPs lecture: functional aspects of the neuronal uptake of noradrenaline. *Trends Pharmacol. Sci.* 32:334–337 (1991).
3. Ramamoorthy, S., P. D. Prasad, P. Kulanthaivel, F. H. Leibach, R. D. Blakely, and V. Ganapathy. Expression of a cocaine-sensitive norepineph-

rine transporter in the human placental syncitiotrophoblast. *Biochemistry* **32:**1346–1353 (1993).
4. Galli, A., L. J. DeFelice, B. J. Duke, K. R. Moore, and R. D. Blakely. Sodium-dependent norepinephrine-induced currents in norepinephrine transporter transfected HEK-293 cells blocked by cocaine and antidepressants. *J. Exp. Biol.*, **198:**2197–2212 (1995).
5. Blakely, R. D., L. J. DeFelice, and H. C. Hartzell. Molecular physiology of norepinephrine and serotonin transporters. *J. Exp. Biol.* **196:**263–281 (1994).
6. Barker, E. L., and R. D. Blakely. Norepinephrine and serotonin transporters: molecular targets of antidepressant drugs, in *Psychopharmacology: The Fourth Generation of Progress*. (F. E. Bloom and D. J. Kupfer, eds.). Raven Press, New York, 321–333 (1995).
7. Pacholczyk, T., R. D. Blakely, and S. G. Amara. Expression cloning of a cocaine- and antidepressant-sensitive human noradrenaline transporter. *Nature (Lond.)* **350:**350–354 (1991).
8. Amara, S. G., and M. J. Kuhar. Neurotransmitter transporters: recent progress. *Annu. Rev. Neurosci.* **16:**73–93 (1993).
9. Shafqat, S., M. Velaz-Faircloth, A. Guadano-Ferraz, and R. T. Fremeau. Molecular characterization of neurotransmitter transporters. *Mol. Endocrinol.* 1517–1529 (1993).
10. Melikian, H. E., J. K. McDonald, H. Gu, G. Rudnick, K. R. Moore, and R. D. Blakely. Human norepinephrine transporter: biosynthetic studies using a site-directed polyclonal antibody. *J. Biol. Chem.* **269:**12290–12297 (1994).
11. Tate, C. G., and R. D. Blakely. The effect of N-linked glycosylation on activity of the Na^+- and Cl^--dependent serotonin transporter expressed using recombinant baculovirus in insect cells. *J. Biol. Chem.* **269:**26303–26310 (1994).
12. Qian, Y., H. E. Melikian, D. B. Rye, A. I. Levey, and R. D. Blakely. Identification and characterization of antidepressant-sensitive serotonin transporter proteins using site-specific antibodies. *J. Neurosci.* **1261:** 1261–1274 (1995).
13. Lew, R., R. Vaughan, R. Simantov, A. Wilson, and M. J. Kuhar. Dopamine transporters in the nucleus accumbens and the striatum have different apparent molecular weights. *Synapse* **8:**152–153 (1991).
14. Patel, A. P., C. Cerruti, R. A. Vaughan, and M. J. Kuhar. Developmentally regulated glycosylation of dopamine transporter. *Dev. Brain Res.* **83:**53–58 (1995).
15. Keynan, S., Y. Suh, B. I. Kanner, and G. Rudnick. Expression of a cloned γ-aminobutyric acid transporter in mammalian cells. *Biochemistry* **31:** 1974–1979 (1992).
16. Zaleska, M. M., and M. Erecińska. Involvement of sialic acid in high-affinity uptake of dopamine by synaptosomes from rat brain. *Neurol. Lett.* **82:**107–112 (1987).
17. Kreienkamp, H.-J., S. M. Sine, R. K. Maeda, and P. Taylor. Glycosylation sites selectively interfere with α-toxin binding to the nicotinic receptor. *J. Biol. Chem.* **269:**8108–8114 (1994).
18. Leconte, I., C. Auzan, A. Deban, B. Rossi, and E. Clauser. N-linked oligosaccharide chains of the insulin receptor β subunit are essential for transmembrane signaling. *J. Biol. Chem.* **267:**17415–17423 (1992).
19. Wu, J.-S. R., and J. E. Lever. N-linked glycosylation is not required for Na^+/glucose symport activity in LLC-PK1 cells. *Biochim. Biophys. Acta* **1192:**289–292 (1994).
20. van Koppen, C. J., and N. M. Nathanson. Site-directed mutagenesis of the m2 muscarinic acetylcholine receptor: analysis of the role of N-glycosylation in receptor expression and function. *J. Biol. Chem.* **265:** 20887–20892 (1990).
21. Gu, H., S. C. Wall, and G. Rudnick. Stable expression of biogenic amine transporters reveals differences in inhibitor sensitivity, kinetics, and ion dependence. *J. Biol. Chem.* **269:**7124–7130 (1993).
22. Sargiacomo, M., M. Lisante, L. Graeve, A. Le Bivic, and E. Rodriguez-Boulan. Integral and peripheral protein composition of the apical and basolateral membrane domains in MDCK cells. *J. Membr. Biol.* **107:**277–286 (1989).
23. Gottardi, C. J., L. A. Dunbar, and M. J. Caplan. Biotinylation and assessment of membrane polarity: caveats and methodological concerns. *Am. J. Physiol.* **268:**F285–F295 (1995).
24. Cheng, Y., and W. H. Prusoff. Relationship between ther inhibition constant (Ki) and the concentration of inhibitor which causes 50 per cent inhibition (I50) of an enzymatic reaction. *Biochem. Pharmacol.* **22:**3099–3108 (1973).
25. Denning, G. M., M. P. Anderson, J. F. Amara, J. Marshall, A. E. Smith, and M. J. Welsh. Processing of mutant cystic fibrosis transmembrane conductance regulator is temperature sensitive. *Nature (Lond.)* **358:**761–764 (1992).
26. Zhu, J., and T. D. Hexum. Characterization of cocaine-sensitive dopamine uptake in PC12 cells. *Neurochem. Int.* **21:**521–526 (1992).
27. Olivares, L., C. Aragon, C. Gimenez, and F. Zafra. The role of *N*-glycosylation in the targeting and activity of the GLYT1 glycine transporter. *J. Biol. Chem.* **270:**9437–9442 (1995).
28. Pedemonte, C. H., G. Sachs, and J. H. Kaplan. An intrinsic membrane glycoprotein with cytosolically oriented N-linked sugars. *Proc. Natl. Acad. Sci. USA* **87:**9789–9793 (1990).
29. Dorner, A. J., and R. J. Kaufman. Analysis of synthesis, processing, and secretion of proteins expressed in mammalian cells. *Methods Enzymol.* **185:**577–596 (1990).
30. Paulson, J. C. Glycoproteins: what are the sugar chains for? *TIBS* **14:**270–276 (1989).
31. Asano, T., K. Takata, H. Katagiri, H. Ishihara, K. Inukai, M. Anai, H. Hirano, Y. Yazaki, and Y. Oka. The role of N-glycosylation in the targeting and stability of GLUT1 glucose transporter. *FEBS Lett.* **324:**258–261 (1993).
31a. Gu, H. H., J. Ahn, M. J. Caplan, R. D. Blakely, A. I. Lerey, and G. Rudnick. Cell-specific sorting of biogenic amine transporters expressed in epithelial cells. *J. Biol. Chem.*, in press.
32. Kanner, B. I. Bioenergetics of neurotransmitter transport. *Biochim. Biophys. Acta* **726:**293–316 (1983).
33. Rudnick, G., and J. A. Clark. From synapse to vesicle: the reuptake and storage of biogenic amine neurotransmitters. *Biochim. Biophys. Acta* **1144:**249–263 (1993).
33a. Galli, A., R. D. Blakely, and L. J. DeFelice. Norepinephrine transporters have channel modes of conduction. *Proc. Natl. Acad. Sci. USA*, in press.
34. Kornfeld, R., and S. Kornfeld. Asparagine-linked oligosaccharides. *Annu. Rev. Biochem.* **54:**631–664 (1995).
35. Bruss, M., R. Hammermann, S. Brimijoin, and H. Bönisch. Antipeptide antibodies confirm the topology of the human norepinephrine transporter. *J. Biol. Chem.* **270:**9197–9201 (1995).
36. Codogno, P., J. Botti, J. Font, and M. Aubery. Modification of the N-linked oligosaccharides in cell surface glycoproteins during chick embryo development. *Eur. J. Biochem.* **149:**453–460 (1985).
37. Lew, R., A. Patel, R. A. Vaughan, A. Wilson, and M. J. Kuhar. Microheterogeneity of dopamine transporters in rat striatum and nucleus accumbens. *Brain Res.* **584:**266–271 (1992).
38. Patel, A., J. Boja, J. Lever, R. Lew, R. Simantov, F. I. Carrol, A. H. Lewin, A. Phillip, Y. Gao, and M. J. Kuhar. A cocaine analog and a GBR analog label the same protein in rat striatal membranes. *Brain Res.* **576:**173–174 (1992).

Send reprint requests to: Randy D. Blakely, Ph.D., Center for Molecular Neuroscience, Vanderbilt University School of Medicine, Nashville, TN 37232-6600. E-mail: randy.blakely@mcmail.vanderbilt.edu